Canadian Science Publishing
NRC Research Press journals | Publishing Services

Canadian Geotechnical Journal
Revue canadienne de géotechnique

Influence of drying-wetting cycles on soil-water characteristic curve of undisturbed granite residual soils and microstructure mechanism by NMR T_2 relaxometry

Journal:	*Canadian Geotechnical Journal*
Manuscript ID	cgj-2016-0614.R1
Manuscript Type:	Article
Date Submitted by the Author:	02-Jun-2017
Complete List of Authors:	Kong, Lingwei; Institute of Rock and Soil Mechanics,Chinese Academy of Sciences, State Key Laboratory of Geomechanics and Geotechnical Engineering Sayem, H. M.; Institute of Rock and Soil Mechanics, Chinese Academy of Sciences, State Key Laboratory of Geomechanics and Geotechnical Engineering; Jahangirnagar University, Department of Geological Sciences Tian, Huihui; Institute of Rock and Soil Mechanics, Chinese Academy of Sciences, State Key Laboratory of Geomechanics and Geotechnical Engineering
Keyword:	Granite residual soil, Drying-wetting cycles, Soil-water characteristic curve (SWCC), Nuclear magnetic resonance (NMR), Pore size distribution (POSD)

Influence of drying-wetting cycles on soil-water characteristic curve of undisturbed granite residual soils and microstructure mechanism by NMR T_2 relaxometry

by

Lingwei KONG*

(*Corresponding Author)

State Key Laboratory of Geomechanics and Geotechnical Engineering

Institute of Rock and Soil Mechanics, Chinese Academy of Sciences, Wuhan 430071,China

Tel: (86)(27)87197521, Fax: (86)(27)87197386, Email: lwkong@whrsm.ac.cn

Hossain Md. SAYEM[1, 2]

1.State Key Laboratory of Geomechanics and Geotechnical Engineering

Institute of Rock and Soil Mechanics, Chinese Academy of Sciences, Wuhan 430071 China

2.Department of Geological Sciences, Jahangirnagar University, Dhaka 1342, Bangladesh

and

Huihui TIAN

State Key Laboratory of Geomechanics and Geotechnical Engineering

Institute of Rock and Soil Mechanics, Chinese Academy of Sciences, Wuhan430071, China

Revised Manuscript Submitted to **Canadian Geotechnical Journal** for possible publication as an article

June 2017

Influence of drying-wetting cycles on soil-water characteristic curve of undisturbed granite residual soils and microstructure mechanism by NMR T_2 relaxometry

by

Lingwei KONG, Hossain Md. SAYEM, and Huihui TIAN

Abstract： Due to the formational environment and climatic variability, granite residual soils with grain size distribution ranging from gravel to clay, are experienced by multiple drying-wetting cycles. The Influences of multiple drying-wetting cycles on the soil-water characteristic curve (SWCC) and pore size distribution (POSD) of undisturbed granite residual soils are investigated using the pressure plate test and nuclear magnetic resonance (NMR) spin-spin relaxation time (T_2) distribution measurement, respectively. The result shows that the water-retention capacity, air entry value decreases and pores become more uniform with increasing drying-wetting cycles. After 4 drying-wetting cycles, the soil reaches to a nearly constant state. The POSD change of multiple drying-wetting cycle samples possesses consistency with the SWCC of the soils. Furthermore, a modified van Genuchten model in terms of cumulative pore volume is used to obtain the best-fit POSD of the drying-wetting cycle samples. The shape and changing tendency of both curves of SWCC and POSD are quite similar and observed a better correlation. It can be concluded that the SWCC is strongly dependent on the POSD of the soil and NMR T_2 relaxometry can be used as an alternative for the assessment of micro-structural variation of residual soils subjected to the periodic drying and wetting process.

Key words: Granite residual soil, Drying-wetting cycles, Soil-water characteristic curve

(SWCC), Nuclear magnetic resonance (NMR), Pore size distribution (POSD).

Introduction

Residual soils are the weathering product of their parent materials. Their engineering properties and behaviors vary widely from place to place depending upon the rock of origin and the local climate during their formation (Fookes 1990). These soils are found in many parts of the world and are used extensively in construction, either to build upon, or as construction material of both geotechnical and geo-environmental structures. The climatic zones where granite residual soils occur are often experienced by seasonal changes in water contents due to water infiltration and evaporation. This climatic variability, namely drying-wetting cycle, is considered to be one of the important factors that can significantly alter moisture distribution and hydro-mechanical behaviors of soils. It may induce damage to foundations or infrastructures. Therefore, it is necessary to evaluate the effects of multiple drying-wetting cycles on the microstructure of natural residual soils.

A significant number of investigations have been conducted to understand the effects of drying-wetting cycles on soil physical and mechanical properties. It is found that soil fabric, particle cementation, water content and void ratio are altered significantly (Cuisinier and Masrouri 2005; Rao and Revanasiddappa 2006; Tripathy et al. 2009; Tovar and Colmenares 2011; Sun and Huang 2015). These effects lead to the formation of cracks as well as the development of fissures in soils, which significantly increase soil compressibility and hydraulic conductivity and consequently decrease the overall structural strength and stability (Morris et al. 1992; Albrecht and Benson 2001; Pires et al. 2008; Li et al. 2009; Sayem et al. 2016). Several researchers also reported that the impact of the first drying-wetting cycle on soil structure is

greatest and decreases with subsequent cycles (Basma et al. 1996; Tripathy et al. 2002; Leij et al. 2002). Bodner et al. (2013) demonstrated that the pore size distribution (POSD) is closely related to cyclic drying-wetting, while overseason dynamics are mainly influenced by soil mechanical disturbance and crop rotation.

The relationship between the water content or degree of saturation and the suction of a soil is generally known as the soil-water characteristic curve (SWCC) and reflects the internal mechanisms of unsaturated soils (Hao et al. 2015). Matric suction is one of the two stresses state variables controlling the behavior of an unsaturated soil, which plays a key role in unsaturated soil mechanics and widely used to predict the hydraulic conductivity, soil water storage and shear strength of unsaturated soils (Fredlund and Rahardjo, 1993). Various methods such as the filter paper method, pressure plate technique, thermal conductivity sensors, tensiometers and thermocouple psychrometers can be used to determine the SWCC. But most of them have some limitations and disadvantages (Kong and Tan 2000. Numerous researchers mentioned that SWCC is influenced by several factors, and each of these factors makes change of pore structure which leads to the change of SWCC. Therefore, the shape of the SWCC is dependent upon the POSD of the soil. Some researchers attempted to obtain the SWCC through the POSD and capillary model (Prapaharan et al. 1985; Olson 1985; Kong and Tan 2000; Aung, et al. 2011; Beckett and Augarde 2013; Zeng, et al. 2013).

Pore size distribution (POSD) is one of the important intrinsic property of soils which is associated with the porosity, void ratio and controls the physical, mechanical and hydraulic behaviors of soils i.e. permeability, storage capacity, shear strength. Several methods are developed to obtain the POSD from porous materials such as the Mercury Intrusion

Porosimetry (MIP), Water Vapour or Nitrogen Adsorption method, X-ray Computer Tomography (CT), Scanning Electron Microscopy (SEM) etc. Many of those methods require sophisticated and costly equipments and well expertise. Some involve a tedious procedure of sample preparation and testing. The limitations of those methods are reported in literature, and some seems insufficient to obtain the full range of POSD of soils covering from very fine to very coarse aprticles (Kate and Gokhale 2006; Wang, et al. 2016). For example, in MIP, high pressure is required for studying small-sized pores which may result in the breaking of cementing bonds and crushing of grains. It is not suitable for soft materials and materials which contain closed pores. While, the adsorption method fails to measure large pores due to the lack of capillary condensation. They cannot be applied to natural state conditions or unconsolidated samples without removing the pore fluid prior to analysis. Desiccation may cause irreversible changes in pore structure, which in turn will affect the actual POSD of the soils. The Image analysis or Microscopy requires approach a large quantity of two-dimensional information for the desired three-dimensional pore structure information and it is time-consuming (Gallegos and Smith 1988; Hinedi et al. 1997; Giesche 2006; Kate and Gokhale 2006; Minagawa, et al. 2008; Benjamini et al. 2014; Wang et al. 2016). None of those methods are suitable for this present study because the tested soil is a special kind of low density (dry density, ρ_d=1.30 g/cm^3) granite residual soil with grain size distribution ranging from gravel to clay.

Nuclear magnetic resonance (NMR) relaxometry is becoming a promising method to evaluate the POSD in soil science. It is possible to overcome those limitations mentioned above. Recently, numerous studies reported the potentiality of NMR relaxometry to assess the POSD of porous media in a fast and non-destructive way (Kleinberg 1994; Strange et al. 1993; Hinedi

et al. 1997; Milia et al. 1998; Dunn et al. 2002; Ramia et al. 2010). It is well known that the amplitude of the proton NMR signal is proportional to the fluid content and that relaxation times give information on the POSD. Though NMR techniques are extensively used in petroleum industry and medical science, recently it has been used successfully in soil mechanics, such as, to quantify and estimate the amount of water in soils, to evaluate porosity, POSD and hydraulic conductivity, to characterize hydraulic processes of unsaturated soils or characterizing the vadose zone and pore water distribution and migration at various sections of hydraulic cycles (Gallegos and Smith 1988; Akporiaye et al. 1994; Strange et al. 1993; Milia et al. 1998; Yun et al. 2002; Bird et al. 2005; He et al. 2005; Mohnke and Yaramanci 2008; Jaeger et al. 2009; Stingaciu et al. 2010; Ramia et al. 2010; Costabel and Yaramanci 2013; Tian et al. 2014; Walsh et al. 2014). NMR technique is also applied to investigate the POSDs of permafrost and gas hydrate sediments (Kleinberg and Griffin 2005; Kleinberg 2006; Tian et al. 2015). Costabel and Yaramanci (2013) studied the estimation of water retention parameters from nuclear magnetic resonance relaxation time distributions. On other hand, Chen et al. (2016) developed a new method for the soil-water retention curve of fine grained soil using NMR technique.

Most of the previous investigations of SWCC are limited to a single drying and wetting cycle or based on multiple drying-wetting cycles on expansive soils, artificial soils and reconstructed soils for the purpose of slope stability analysis, soil stabilization or for the study of contaminant transport, nuclear waste disposal barrier, dam, etc. The effects of multiple drying-wetting cycles on SWCC of undisturbed granite residual soils are still far from being well understood. The main objective of this study is to evaluate the effects of multiple

drying-wetting cycles on SWCC of undisturbed granite residual soils. The variations of POSD also analyzed using the NMR T_2 technique. Such studies will be useful to understand the possible micro-structural variations of granite residual soils subject to a periodic drying and wetting process.

Theoretical background of NMR T_2

The NMR signal is an exponential decay, characterized by initial signal amplitude and distribution of relaxation times (T_2). The NMR signals are generated from liquids when the sample is placed in a magnetic field and then excited with a brief pulse of radio frequency (RF) energy. The signal amplitude is an indication of total fluid present or related to characteristic pore abundance while the relaxation time (T_2) is a measure of the rate at which the precession of hydrogen nuclei in the formation pore fluid gradually decay in the presence of an inhomogeneous magnetic field, which give information on the POSDs. According to Coates et al. (1999), for a fluid saturated porous media (e.g. soil/rock), the NMR relaxation mechanisms are given by

$$\frac{1}{T_2} = \frac{1}{T_{2B}} + \frac{1}{T_{2S}} + \frac{1}{T_{2D}} \quad (1)$$

Where, T_2 is the transverse relaxation time of the pore fluid as measured by a Carr-Purcell-Meiboom-Gill (CPMG) sequence; T_{2B} is the transverse bulk fluid relaxation time; T_{2S} is the transverse surface relaxation time; T_{2D} is the diffusion relaxation time and accounts for the transverse relaxation in an inhomogeneous magnetic field.

It is reported that the NMR relaxation of water saturated sedimentary rock or unconsolidated sediments occurs in the fast-diffusion regime and that there is little or no pore

coupling (Brownstein and Tarr 1979; Kenyon 1997; Dunn et al. 2002). T_{2B} is typically much larger than T_{2S} and the effect of T_{2D} is minor for CPMG pulse sequence (Yun et al. 2002; Lao 2010; Behroozmand et al. 2015). Furthermore, at low field NMR, both T_{2B} and T_{2D} are negligible compared to T_{2S} (Kleinberg 2006). Therefore, in the fast diffusion limit, the transverse relaxation time (T_2) depends on the transverse surface relaxation (T_{2S}) and the T_2 relaxation rate $1/T_2$ is proportional to the surface-to-volume (S/V) ratio of the pore (Brownstein and Tarr 1979, Godefroy et al. 2001; Tian et al. 2014; Behroozmand et al. 2015). Hence, the equation is

$$\frac{1}{T_2} = \frac{1}{T_{2S}} = \rho_2 \left(\frac{S}{V} \right)_{pore} \tag{2}$$

Where, ρ_2 is the surface relaxivity coefficient, which is a characteristics of magnetic interactions at the fluid-solid interface and $(S/V)_{pore}$ is the ratio of the pore surface area S to the pore water volume V and related to the pore diameter (D), i.e. $(S/V)_{pore} = F_s/D$. The geometry factor, F_s, depends on the pore shape, which assumes a value of 2, 4 and 6 for planar, cylindrical and spherical pores, respectively. For cylindrical pores (Tian et al. 2014), the equation is

$$\frac{1}{T_2} = \rho_2 \frac{4}{D} \tag{3}$$

Therefore, the distribution of relaxation time is linearly proportional to the POSD i.e. short relaxation times correspond to small pores and long relaxation times correspond to large pores. After knowing the value of surface relaxivity coefficient (ρ_2), one can estimate the POSD using Eq. 3. It is important to note that the coefficient surface relaxivity (ρ_2) is normally assumed to be constant when interpreting NMR data. The coefficient ρ_2 is attributed to the paramagnetic

impurities on the surface of the grains that interact with hydrogen nuclei and impose an additional relaxation (Korringa 1962) and the value is constant for a particular soil and depends on the specific combination of mineral grain and pore fluid (Tian et al. 2014).

Materials and methods

Physical characteristics of the soil

The undisturbed granite residual soil samples collected at areas (5.0-7.0 m depth) around Jiangmen city (Kaiping), Gaungdong province, China, are used for this study. According to X-ray diffraction analysis, the soils are mainly composed of kaolinite with small amount of illite, the non-clay minerals include quartz, pyrite and gibbsite (Sayem et al. 2016). The basic material properties are measured in the laboratory and given in table 1, and its grain size distribution is shown in Fig. 1.

Drying-wetting sample preparation

In the preparation procedure, the samples with 20mm in height and 61.8mm in diameter for the pressure plate test and 20mm in height and 45mm in diameter for the NMR test are obtained by cutting the core samples using cutting ring. After weighting, the samples are dried up to moisture content 20% at constant temperature of 40 ± 2 °C (the highest temperature under simulated natural conditions) for 24 h using temperature and humidity control box. Remove the specimens from oven and allow 1-2 h for cooling at the room temperature (around 20 °C). The samples are covered by the filter paper and water-permeable stone both on the top and bottom to prevent any disturbance during the saturation process. Then the samples are saturated with

distilled water after vacuum seeding about 2 hours and then submerged about 24h. Later the samples are dried up to 20% moisture content in the oven at constant temperature of 40 ± 2 °C. This is called as one drying-wetting cycle. This process is repeated until the desired numbers of drying-wetting cycles (0, 1, 2, 4 and 8) are completed.

Experimental methods

Tests are conducted on saturated samples experienced by drying-wetting cycles (0, 1, 2, 4 and 8). The SWCCs of those samples are obtained using a pressure plate apparatus produced by Soil Moisture Equipment Corporation of USA (Fig. 2). This apparatus adopts the principle of axis translation technique. Experiments are performed based on the reference, ASTM 6836-02 (2002). The entire SWCC and the corresponding fitting parameters are obtained by using the van Genuchten (1980) model. This model is most popular and well accepted for SWCC determination as well as can predict the residual water content more perfectly. The mathematical formula is

$$\theta = \theta_r + \frac{\theta_s - \theta_r}{[1 + (\alpha\psi)^n]^m} \quad (4)$$

Where, ψ is the suction pressure (kPa) i.e (u_a-u_w), θ is the volumetric water content，θ_s is the saturated water content, θ_r is the residual water content, α, n & m are soil parameters. In which，α is the inverse of the air-entry pressure, n is the parameter on the pore size distribution and m=1-1/n.

The POSD is analyzed in terms of T_2 distribution using a 23 MHz MiniMR NMR, jointly developed by the Institute of Rock and Soil Mechanics, Chinese Academy of Sciences, and Niumag Corporation, Suzhou, Jiangsu Province, China (Fig. 3). The system consists of a

sample tube, magnet unit, radio-frequency (RF) system, temperature controlling system and data acquisition-analysis system. To generate a stable and uniform magnetic field, the temperature of the magnet unit is set to be 32 °C, within a variation of ±0.01 °C. For the determination of T_2 relaxation time, the Carr-Purcell-Meiboom-Gill pulse sequence is employed to minimize the effect of magnetic field inhomogeneities on the NMR signal. The detailed method for measuring the T_2 distribution curves is given in the literature (Tian et al. 2014).

Determination of Surface Relaxivity coefficient (ρ_2)

Several attempts have been undertaken to estimate the value of ρ_2. Some researches obtained ρ_2 values by comparing the T_2 relaxation distribution with POSD data calculated by MIP (Marschall et al. 1995; Kleinberg 1996; Kenyon 1997; Li et al. 2008; Minagawa, et al. 2008; Yao and Liu 2012), Nitrogen Gas Adsorption or Diffusion measurements (Gallegos and Smith 1988; Hurlimann et al. 1994; Sorland et al. 2007), Cation Exchange Capacity (Sen et al. 1990), Differential Thermal Calorimetry (Ramia et al. 2010) and Photo Microscopy or Image Analysis (Howard et al. 1993; Kenyon 1997; Arns 2004; Wang 2009) techniques. Some are also calculated ρ_2 by using empirical formula of hydraulic conductivity such as the Hazen formula or the Kozeny-Carmann approximation (Kenyon et al. 1988; Kenyon 1992; Straley et al. 1994; Yun et al. 2002; He et al. 2005, Daigle and Dugan 2009). In this research, a well accepted NMR-permeability equation, known as Schlumberger-Doll Research (SDR) equation developed by Kenyon et al. (1988), is used to obtain the surface relaxivity coefficient (ρ_2) which is

$$k_s = C\Phi^4 T_{2LM}^2 \quad (5)$$

According to Kleinberg et al. (2003), the constant C of SDR equation is expected to be

proportional to the square of the surface relaxivity coefficient i.e $C = \rho_2^2$,which depends on mineralogy and magnetic impurities (For details see Daigle and Dugan 2009).Therefore, The equation is as follows:

$$k_s = \rho_2^{\,2}\, \Phi^4\, T_{2LM}^2 \tag{6}$$

It can also be written as

$$\rho_2 = \sqrt{k_s\, \Phi^4\, T_{2LM}^2} \tag{7}$$

Where, k_s is the saturated permeability of the soils (m^2) which is measured by virgin portion of the consolidation curve (k_s=9.91×10^{-16} m^2); Φ is the saturated porosity of the NMR samples (Φ=0.5006); T_{2LM} is the geometric mean value of the T_2 distribution (T_{2LM}=0.86534 ms).The obtained ρ_2 value is about 0.1452μm/ms.

Results and discussions

Pressure Plate test results

The matric suction is measured by pressure plate extractors in this research. The variations of water content with respect to matric suction of drying-wetting cycle samples are shown in Fig. 4. The entire fitting curves and corresponding SWCC parameters of drying-wetting soil samples are shown in Fig. 5 and table 2 respectively. The results show that the initial saturated water content and residual water content decreases with increasing drying-wetting cycles i.e. the water-retention capacity decreases. This may be due to the breakdown of bonding structures, decrease of pore volume and formation of cracks with increasing alternate drying-wetting cycles (Sayem and Kong 2016). During the drying-wetting cycles, cracks induced by drying

process. With increasing cycle numbers, the existing cracks are enlarged as well as new cracks are developed, resulting in the formation of abundant shrinkage cracks. The values of α and n increase with increasing drying-wetting cycles, whereas the value of m decreases (table 2). The air entry value is inversely proportional to α, therefore, the air entry value is 40.3kPa,35.8kPa,33.1kPa,31.5kPa,31.4kPa for 0, 1, 2, 4 and 8 cycles respectively, and decreases with increasing drying-wetting cycles. In addition, larger value of n indicates more uniform pore sizes with dry-wetting cycles. It is found that the SWCC shifts to the left with increasing drying-wetting cycles and reaches to a nearly constant state after 4 cycles of drying-wetting. However, after 4 drying-wetting cycles, the soil behaves like a passive system and it does not allow further moisture adsorption or desorption. To clarify the SWCC results, the POSD of multiple drying-wetting cycle samples is examined using NMR T_2 relaxometry.

NMR T_2 test results

The relaxation time distributions are normalized to the sum of all amplitudes; each amplitude then represents the proportion of water corresponding to its relaxation time (the decay of the NMR signal). The distribution curves of transverse relaxation times T_2 of saturated drying-wetting cycle samples of granite residual soils from NMR experiments are shown in Fig. 6 where the results show bimodal relaxation distributions. As the short relaxation times correspond to small pores and long relaxation times correspond to large pores, the bimodal relaxation distributions indicate the existence of macro- and micropores in the soil particles. The comparison of the distribution curves for the NMR T_2 results shows that the NMR signal proportion decreases with increasing drying-wetting cycles. The variations of the peak area (the signal amplitude of the T2 distribution curve which represents the population of water

molecules or the amount of water content in the pores) and T_2 at peak (the value of T_2 at the maximum NMR signal) with respect to number of drying-wetting cycles are shown in Fig. 7. The reducing rate of total area is 15.96%, 26.73%, 33.64%, 34.09% for 1, 2, 4 and 8 cycles respectively, and the reducing rates from cycle 0→1, 1→2, 2→4 and 4→8 are about 15.96%, 12.82%, 9.42% and 0.69%, respectively. It is seen that the reduction rate is more pronounced in the first cycle and decreases with subsequent cycles and finally reaches to a nearly constant state after 4 cycles. Since the peak area represents the saturated water content of the specimen, the above observation implies that the water retention capacity decreases with increasing drying-wetting cycles. The maximum peak locates at 6.29 ms for the initial sample (C-00). With increasing drying-wetting cycles, the maximum peak value of NMR T_2 (peak 1) are decreased to 5.81 ms, 5.35 ms, 4.94 ms and 4.94 ms for cycle number 1, 2, 4 and 8, respectively i.e. the value of NMR T_2 at peak shifts slightly to the left with increasing drying-wetting cycles in Fig. 7.

POSD from NMR T_2

It is well known that the NMR signal amplitude is proportional to the fluid content or related to pore abundance and the relaxation times are linearly proportional to the pore size. From the relaxation time distributions, the POSDs of drying-wetting cycle samples calculated using Eq. 3 with ρ_2 value of 0.1452μm/ms given in Fig. 8. The results show that the pore spaces bimodal distribution of cyclic drying-wetting soil samples mainly consist of pores diameter range from 0.0001~55μm. With increasing drying-wetting cycles, the maximum value of Peak 1 are at 0.366μs, 0.337μs, 0.311μs, 0.287μs and 0.287μs for cycle number 0,1, 2, 4 and 8 respectively, while for Peak 2 they are at 13.994μs, 10.975μs, 5.294μs, 4.883μs and 4.883μs,

respectively. Therefore, the optimal pore diameter decreases with increasing drying-wetting cycles which is more obvious for peak 2 with large pore diameter. This may be due to the slaking behaviour and redistribution of water from coarse pores to finer pores.

According to the shape and feature of the pore size distribution curve (Fig. 8), the pore can be preliminarily divided into five different grades by the pore diameter: i) >10μm, ii) 10~5μm, iii) 5~1μm, iv) 1~0.1μm and v) <0.1μm). The corresponding results are summarized in Table 3. It can be observed that the pores ranging from 5~1μm constitute the majority of the pore space in all samples and compose approximately 50.75% of the total pores. The fractions of pores ranging from >10μm, 10~5μm, 1~0.1μm and <0.1μm are about 5.60%, 15.31%, 25.64% and 2.71%, respectively. All the pores decrease with increasing drying-wetting cycles, but the effects of drying-wetting cycles are more predominant for large pores whose diameter >1μm (Fig. 9). For large pores (>10μm), the reduction of pore volume from initial volume is 36.04%, 54.03%, 65.88% and 67.30% for 1, 2, 4 and 8 cycles respectively, whereas it is about 8.24%, 13.58%, 18.25% and 18.82% for pores ranging from 1-0.1μm. During the drying-wetting cycle-1, the reduction of pore distribution from the initial value is about 2.61%, 8.24%, 15.46%, 19.60% and 36.04% for pores <0.1μm, 1~0.1μm, 5~1μm, 10~5μm and >10μm, respectively. It is found that the effect of drying-wetting cycles on larger pores is more obvious than smaller pores. From table 3, it can also be seen that the impact of drying-wetting cycles on POSD is more apparent in the first cycle and decreases with subsequent cycles. After 4 drying-wetting cycles, there is no significant change in T_2 as well as POSDs. Therefore, it seems that the particles are unable to move for further drying-wetting cycles and the pores become rigid.

The obtained POSD of the drying-wetting cycle samples are fitted with the van Genuchten

(1980) model in terms of the cumulative pore volume (mm^3/g) where the suction is replaced by the pore diameter. The mathematical formula is

$$V_{Di} = V_r + \frac{V_s - V_r}{[1 + (a / D_i)^b]^c} \quad (8)$$

Where, V_{Di} is the cumulative pore volume less than pore diameter D_i (μm), V_s is the saturated pore volume, V_r is the residual pore volume and a, b & c are empirical constants related to the solid phase characteristics.

The predicted POSD curves and their fitting parameters are given in Fig. 10 and table 4 respectively. It can be seen that the value of residual pore volume (V_r) is very small corresponding to the saturated pore volume (V_s), and is very close to 0. Based on regression analysis, it is found that the correlation coefficient of the fitting curves increased much better if the residual pore volume is considered as 0. Therefore, Eq. 8 is modified considering V_r equal to 0 and without changing the other fitting parameters. The modified equation is

$$V_{Di} = \frac{V_s}{[1 + (a / D_i)^b]^c} \quad (9)$$

Using modified van Genuchten (1980) model in terms of cumulative pore volume (mm^3/g) and pore diameter (Eq. 7), the obtained POSD fitting curves and corresponding fitting parameters are shown in Fig. 11 and table 5 respectively.

Discussion

For comparison among the fitting parameters of SWCC and POSD, the relationship between α and a is taken as an example, where the parameter α has units of soil suction or the inverse of soil suction and inversely related to the air entry value and the parameter a has units of pore diameter. According to the Washburn (1921) equation, the equivalent pore diameters

for the values of α are found to range from 7.1 to 9.1μm. On the other hand, the threshold pore diameters a for NMR test are range from 6.7 to 7.0μm. This finding shows that the pore diameter at the threshold level of NMR T_2 test and the air entry value of the SWCC are reasonably related and the first drainage occurs later for T_2 POSD. The variations among the fitting parameters may be caused by several reasons- (i) the natural variability and inhomogeneity of the soil, (ii) the relationship between two different physical properties and the inverse relationship between suction pressure and pore size, (iii) the different accuracy of measurement for pressure plate and NMR T_2 as well as variations of sample size, (iv) transformational errors of relaxation distribution functions in POSD cumulative functions and (v) the disturbance of soil structures during sample collection and preparation. Furthermore, the shrinkage cracks are expected during desiccation process in pressure plate test which may also be a reason for these variations.

Through investigating the relation of the fitting parameters α, n & m and a, b & c, it can be seen that there is a good correlation between fitting parameters for SWCC and POSD, i.e. the fitting parameters are linearly proportional to each other (Fig. 12). It is quite well known that the POSD curve is intrinsically related to the SWCC. Therefore, the linearity of the relationship between fitting parameters in SWCC and POSD is said to be attributed to the similarity of the physical meaning of the parameters for the studied soil. For example, the POSD fitting parameter a is the threshold pore diameter indicating the inflection point on the curve which inversely proportional to the air entry value. The shape and changing tendency of SWCC and POSD curves are quite similar. Furthermore, from table 2 & 4, it is found that the cumulative pore volume of 0.1μm pore diameter is very close to the equivalent residual water content (θ_r/ρ_d)

of SWCC which might be the clay-bound water. Though SWCC is influenced by several factors, from this study it can be concluded that the SWCCs of drying-wetting cycles are strongly affected by the POSD of the soil and NMR T_2 relaxometry can be used as a fast and very simple alternative for the assessment of pore size distribution.

Conclusion

In this paper, the effects of multiple drying-wetting cycles on SWCC of undisturbed granite residual soils are investigated using the pressure plate test and their POSDs are examined through NMR T2 relaxometry. The water-retention capacity of undisturbed granite residual soils decreases with increasing drying-wetting cycles i.e. the initial saturated water content, residual water content and air entry value decrease. The impact of first drying-wetting cycle is more apparent on SWCC and decreases with subsequent cycles; the soil reaches to a nearly constant state after 4 drying-wetting cycles. The NMR T_2 relaxometry can be used as an alternative for the assessment of POSD of granite residual soils with grain size distribution ranging from gravel to clay. Moreover, the obtained POSD of multiple drying-wetting cycle samples are consistency with the SWCC of the soils, and the cumulative pore volume of POSD can be well described by the formula of modified van Genuchten model. The shape and changing tendency of the both curves of SWCC and POSD of granite residual soils with increasing drying-wetting cycles are quite similar and observed a better correlation i.e. the fitting parameters of SWCC and POSD are linearly proportional to each other. Therefore, the SWCC change of soils is strongly depend on the initial POSD and its alteration with multiple drying-wetting cycles.

ACKNOWLEDGEMENT

The authors would like to acknowledge financial support from the National Natural Science Foundation of China (Grant No. 41372314， 11672320) and the Science and Technology Service Network Initiative of the Chinese Academy of Sciences (Grant No. KFJ-EW-STS-122).

REFERENCES

Akporiaye, D., Hansen, E.W., Schmidt, R. and Stocker, M. 1994. Water-saturated mesoporous MCM-41 systems characterized by ^{1}H NMR, Jour Phys Chem, 98 (7), 1926-1928.

Albrecht, B.A. and Benson, C.H. 2001. Effect of desiccation on compacted natural clays, Journal of Geotechnical and Geoenvironmental Engineering, 127, 67-75.

Arns, C.H. 2004. A comparison of pore size distributions derived by NMR and X-ray CT techniques. Physica A, 339, 159-165.

ASTM D6836-02, 2002. Methods for Determination of the Soil Water Characteristic Curve for Desorption Using Hanging Column, Pressure Extractor, Chilled Mirror Hygrometer, or Centrifuge, ASTM International, West Conshohocken, PA.

Aung, K.K., Rahardjo, H., Leong, E.C., and Toll, D.G. 2011. Relationship between porosimetry measurement and soil-water characteristic curve for an unsaturated residual soil. Geotechnical and Geological Engineering, 19, 401-416.

Basma, A.A., Al-Homoud, A.S., Husein Malkawi, A.I., and Al-Bashabsheh, M.A. 1996. Swelling-shrinkage behavior of natural expansive clays, Appl Clay Sci, 11, 211-227.

Beckett, C.T.S., and Augarde, C.E. 2013. Prediction of Soil Water Retention properties using pore-size distribution and porosity. Can. Geotech. J., 50, 435-450.

Behroozmand, A.A., Keating, K., and Auken, E. 2015. A Review of the Principles and Applications of the NMR Technique for Near-Surface Characterization. Survey in Geophysics, 36(1), 27-85.

Benjamini, D., Elsner, J.J., Zilberman, M., and Nevo, U. 2014. Pore size distribution of bioresorbable films using a 3-D diffusion NMR method. Acta Biomaterialia, 10(6), 2762-2768. doi:10.1016/j.actbio.2014.02.014

Bird, N.R.A., Preston, A.R., Randall, E.W., Whalley, W.R., and Whitmore, A.P., 2005. Measurement of the size distribution of water-filled pores at different matric potentials by stray field nuclear

magnetic resonance, European Journal of Soil Science, 56, 135-143.

Bodner, G., Scholl, P., and Kaul, H.P. 2013. Field quantification of wetting-drying cycles to predict temporal changes of soil pore size distribution, Soil & Tillage Research, 133, 1-9.

Brownstein K.R. and Tarr C.E. 1979. Importance of classical diffusion in NMR studies of water in biological cells, Physical Review, 19 (6), 2446-2453.

Chen, P., Wei, C.F., and Liu, J. 2015. Evolution of soil water in silt soils based on NMR technique. In: Chen, et al. (eds), Proceedings of the 6th Asia-pacific Conference on Unsaturated soils, Taylor & Francis Group, London, 181-184.

Coates, G.R., Xiao, L., and Prammer, M.G. 1999. NMR Logging Principles and Applications. Halliburton Energy Services, Houston.

Costabel, S., and Yaramanci, U. 2013. Estimation of water retention parameters from nuclear magnetic resonance relaxation time distributions. Water Resources Research, 49, 2068-2079. doi:10.1002/wrcr.20207.

Cuisinier, O., and Masrouri, F. 2005. Hydromechanical behavior of a compacted swelling soil over a wide suction range. Eng Geol, 81, 204-212.

Daigle, H., and Dugan, B. 2009. Extending NMR data for permeability estimation in fine-grained sediments. Marine and Petroleum Geology, 26, 1419-1427.

Dunn, K., Bergman, D.J., and Latorraca, G.A. 2002. Nuclear Magnetic Resonance- Petrophysical and Logging Applications, Elsevier Sci., Oxford, UK.

Fookes, P.G. 1990. Report on tropical residual soils. Quart Jour Eng Geol, 23, 103-108.

Fredlund, D.G., and Rahardjo, H. 1993. Soil mechanics for unsaturated soils, John Wiley, New York.

Gallegos, D.P., and Smith, D.M. 1988. A NMR Technique for the Analysis of Pore Structure: Determination of Continuous Pore Size Distributions, Journal of Colloid and Interface Science, 122 (1), 143-153.

Godefroy, S., Korb, J.P., Fleury, M., and Bryant, R.G. 2001. Surface nuclear magnetic relaxation and dynamics of water and oil in macroporous media, Phys Rev E Stat Nonlinear Soft Matter Phys., 64, 216051-2160513.

Hao, D.R., Liao, H.J., Ning, C.M., and Shan, X.P. 2015. The microstructure and soil-water characteristic of unsaturated loess, In: Chen, et al. (Eds.), Proceedings of the 6th Asia-pacific Conference on Unsaturated soils, Taylor & Francis Group, London, 163-167.

He, Y.D., Mao, Z.Q., Xiao, L.Z., and Ren, X.J. 2005. An improved method of using NMR distribution to evaluate pore size distribution. Chinese Journal of Geophysics, 48(2), 373-378 (In Chinese).

Hinedi, Z.R., Chang, A.C., and Anderson, M.A. 1997. Quantification of microporosity by nuclear resonance relaxation of water imbibed in porous media. Water Resour. Res. 33(12), 2697-2704.

Howard, J.J., Kenyon, W.E., and Straley, C. 1993. Proton magnetic resonance and pore size variations in reservoir sandstones. SPE Formation Evaluation, 8(3), 194-200.

Hurlimann, M.D., Helmer, K.G., Latour, L.L., and Sotak, C.H. 1994. Restricted diffusion in sedimentary rocks: Determination of surface-area-to-volume ratio and surface relaxitivity. Journal of Magnetic Resonance, Series A, 111(2), 169-178.

Jaeger, F., Bowe, S., van As, H., and Schaumann, G.E. 2009. Evaluation of ^{1}H NMR relaxometry for the assessment of pore size distribution in soil samples, Eur J Soil Sci, 60(6), 1052-1064.

Kate, J.M., and Gokhale, C.S. 2006. A simple method to estimate complete pore size distribution of rocks. Engineering Geology, 84, 48-69.

Kenyon, W. E. 1992. Nuclear magnetic resonance as a petrophysical measurement, Nucl. Geophys., 6, 153-171.

Kenyon, W.E. 1997. Petrophysical principles of applications of NMR logging. Log Analysis, 38(2), 21-43.

Kenyon, W.E., Day, P.I., Straley, C., and Willemsen, J.F. 1988. A three-part study of NMR longitudinal relaxation properties of water-saturated sandstones. SPE Formation Evaluation, 3(3), 622-636.

Kleinberg, R.L. 1996. Utility of NMR T2 distributions, connection with capillary pressure, clay effect, and determination of the surface relaxivity parameter, ρ_2. Magnetic Resonance Imaging, 14(7-8), 761-767.

Kleinberg, R.L. 2006. Nuclear magnetic resonance pore-scale investigation of permafrost and gas hydrate sediments. In: Rothwell, R.G. (eds.), New Techniques in Sediment Core Analysis.Geological Society, London, Special Publications, 267, 179-192.

Kleinberg, R.L. 1994, Pore size distributions, pore coupling and transverse relaxation spectra of porous rocks, Magnetic Resonance Imaging, 12, 271-274.

Kleinberg, R.L., and Griffin, D.D. 2005. NMR measurements of permafrost: Unfrozen water assay, pore-scale distribution of ice, and hydraulic permeability of sediments, Cold Reg. Sci. Technol., 42, 63-77.

Kleinberg, R.L., Flaum, C., Griffin, D.D., Brewer, P.G., Malby, G.E., Peltzer, E.T., and Yesinowski, J.P. 2003. Deep sea NMR: Methane hydrates growth habit in porous media and its relationship to hydraulic permeability, deposit accumulation, and submarine slope stability. Journal of Geophysical Research, 108(B10), 2508. doi:10.1029/2003JB002389.

Kong, L.W., and Tan, L.R. 2000. A simple method of determining the soil-moisture characteristic curve indirectly. In: Rahardjo, H., Toll, D.G. & Leong, E.C. (eds.), Unsaturated Soils For Asia, Singapore, Balkema, Rotterdam, 341-345.

Korringa, J., Seevers, D.O., and Torrey, H.C. 1962. Theory of spin pumping and relaxation in systems with a low concentration of electron spin resonance centers, Phys. Rev., 127(4), 1143–50.

Lao, U.H. 2010. Wettability measurements by Nuclear Magnetic Resonance. PhD Thesis, University of Stavanger, Norway.

Leij, F.J., Ghezzehei, T.A., and Or, D. 2002. Modelling the dynamics of the soil pore-size distribution, Soil and Tillage Research, 64, 61-78.

Li, H.B., Zhu, J.U., and Guo, H.K. 2008. Methods of calculating pore radius distribution in rock from NMR T_2 spectra. Chinese Journal of Magnetic Resonance, 25(2), 273-280 (In Chinese).

Li, L., Zhu, W., Lin, C., and Ohki, T. 2009. Study of wet and dry properties of solidified sludge, Rock and Soil Mechanics, 30(10), 3001-3004 (in Chinese).

Marschall, D., Gardner, J.S., Mardon, D., and Coates, G.R. 1995. Method for correlating NMR relaxometry and mercury injection data. In: Society of core analysis conference, SCA 9511.

Milia, F., Fardis, M., Papavassiliou, G., and Leventis, A. 1998. NMR in porous materials, Magn Reson Imaging, 16 (5/6), 677-678.

Minagawa, H., Nishikawa, Y., Ikeda, I., Miyazaki, K., Takahara, N., Sakamoto, Y., Komai, T., and Narita, H. 2008. Characterization of sand sediment by pore size distribution and permeability using proton nuclear magnetic resonance measuremen. Journal of Geophysical Research, 113, B07210, doi:10.1029/2007JB005403.

Mohnke, O., and Yaramanci, U. 2008. Pore size distributions and hydraulic conductivities of rocks derived from magnetic resonance sounding data using multi-exponential decay time inversion, J. Appl. Geophys., 66, 73-81.

Morris, P.H., Graham, J., and Williams, D.J. 1992. Cracking in drying soils, Can. Geotech. J. 29, 263–277.

Olson, K.R. 1985. Characterization of Pore Size Distribution within Soils by Mercury Intrusion and Water –release Methods. Soil Science, 139(5), 400-404.

Pires, L.F., Cooper, M., Cássaro, F.A.M., Reichardt, K., Bacchi, O.O.S., and Dias, N.M.P. 2008. Micromorphological analysis to characterize structure modifications of soil samples submitted to wetting and drying cycles, Catena, 72, 297-304.

Prapaharan, S., Altschaeffl, A.G., and Dempsey, B.J. 1985. Moisture Curve of Compacted Clay: Mercury Intrusion Method, Journal of Geotechnical Engineering, 111(9), 1139-1142.

Ramia, M.E., Jeandrevin, S., and Martín, C.A. 2010. Porosity and Pore Size Study by Means of Nuclear Magnetic Resonance and Calorimetry, Ann. Magn. Reson. 9 (2/3), 30-37.

Rao, S.M., and Revanasiddappa, K. 2006. Influence of cyclic wetting drying on collapse behavior of compacted residual soil. Jour Geotech Geol Eng, 24, 725-734.

Sayem, H.M., and Kong, L.W. 2016. Effects of drying-wetting cycles on soil-water characteristic curve, In Proceedings of the 2016 International Conference on Power Engineering & Energy, Environment (PEEE 2016)- Shanghai, China, DEStech publications, Inc, 607-614.

Sayem, H.M., Kong, L.W., and Yin, S. 2016. Effect of Drying-Wetting Cycles on Saturated Shear Strength of Undisturbed Residual Soils. American Journal of Civil Engineering, 4(4), 143-150.

Sen, P.N., Straley, C., Kenyon, W.E., and Whittingham M.S. 1990. Surface-to-volume ratio, charge density, nuclear magnetic relaxation, and permeability in clay-bearing sandstones. Geophysics, 55(1), 61-69.

Sorland, G.H., Djurhuus, K., Wideroe, H.C., Lien, J.R., and Skauge A. 2007. Absolute pore size

distribution from NMR. Diffusion Fundamentals, 5, 4.1-4.15.

Stingaciu, L. R., Weihermüller, L., Haber-Pohlmeier, S., Stapf, S., Vereecken, H., and Pohlmeier, A. 2010, Determination of pore size distribution and hydraulic properties using nuclear magnetic resonance relaxometry: A comparative study of laboratory methods, Water Resour. Res., 46, W11510, doi:10.1029/2009WR008686.

Straley, C., Rossini, D., Vinegar, H., Tutunjian, P., and Morriss, C. 1994. Core Analysis by Low Field NMR, In: Proceedings 1994 International Symposium of the Society of Core Analysts Paper, SCA-9404, 43-56.

Strange, J.H., Rahman, M., and Smith, E.G. 1993. Characterization of porous solids by NMR, Phys Rev Lett, 71(21), 3589-3591.

Sun, D.A., and Huang, D.J. 2015. Soil-water and deformation characteristics of Nanyang expansive soil after wetting-drying cycles. Rock and Soil Mechanics, 36, 115-119. DOI: 10.16285/j.rsm. 2015.S1.019. (in Chinese)

Tian, H., Wei, C., Wei, H., Yan, R., and Chen, P. 2014. An NMR-Based Analysis of Soil-Water Characteristics, Appl Magn Reson, 45, 49-61.

Tian, H., Wei, C., Xia, X., and Wang, H. 2015. Nuclear Magnetic Resonance assay of carbon dioxide hydrate in silt. In: Chen, et al. (eds), Proceedings of the 6th Asia-pacific Conference on Unsaturated soils, Taylor & Francis Group, London, 177-180.

Tovar, R.D., and Colmenares, J.E. 2011. Effects of drying and wetting cycles on the shear strength of argillaceous rocks. In: Alonso, E. E. & Gens, A. (eds.), Proceedings of the 5th international conference on unsaturated soils, Taylor & Francis Group, London, 1471-1476.

Tripathy, S., Kanakapura, S., and Rao, S. 2009. Cyclic swell-shrink behavior of a compacted expansive soil, Geotech Geol Eng, 27, 89-103.

Tripathy, S., Subba Rao, K.S., and Fredlund, D.G. 2002. Water content-void ratio swell-shrink paths of compacted expansive soils, Canadian Geotechnical Journal, 39, 938-959.

Van Genuchent, M.T. 1980. A Closed Form Equation for Prediction of the Hydraulic Conductivity of Unsaturated Soils, Soil Sci. Society America Jour., 44, 892-898.

Walsh, D., Grunewald, E.D., Turner, P., Hinnell, A., and Ferre, T.P.A. 2014. Surface NMR instrumentation and methods for detecting and characterizing water in the vadose zone. Near Surface Geophysics, 12(2), 271-284.

Wang, M., Pande, G., Kong, L., and Feng, Y. 2016. Comparison of Pore-Size Distribution of Soils Obtained by Different Methods. International Journal of Geomechanics, 10.1061/(ASCE)GM. 1943-5622. 0000696, 06016012.

Wang, S. 2009. Analysis of Rock Pore Structural Characteristic by Nuclear Magnetic Resonance, Nanjiang Petrolium Geology, 30(6), 768-770 (In Chinese).

Washburn, E.W. 1921, The dynamics of capillary flow, Phys. Rev., 17, 273-283.

Yao, Y., and Liu, D. 2012. Comparison of low-field NMR and mercury intrusion porosimetry in

characterizing pore size distributions of coals. Fuel, 95(5), 152-158.

Yun, H.Y., Zhao, W.J., Liu, B.K., Zhou, C.C., and Zhou, F.M. 2002. Researching rock pore structure with T_2 distribution. Well Logging Technology, 26(1), 18-21. (In Chinese).

Zeng, Z.T., Lu, H.B., Zhao, Y.L., and Wang Z.B. 2013. Study of pore size distribution of expansive soil during wetting-drying cycle and its application. Rock and Soil Mechanics, 34(2), 322-328 (In Chinese).

List of figures

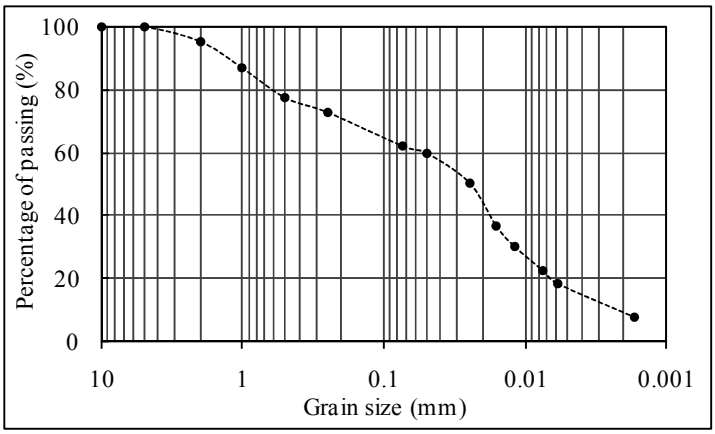

Fig 1. Grain size distribution of the tested granite residual soil

Fig 2. 15 bar Pressure Plate Extractor.

Fig 3. 23 MHz MiniMR NMR.

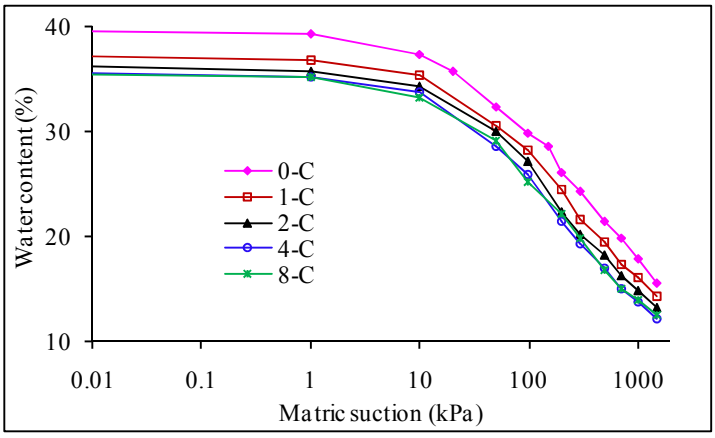

Fig 4. SWCC curves of samples experienced by drying-wetting cycles.

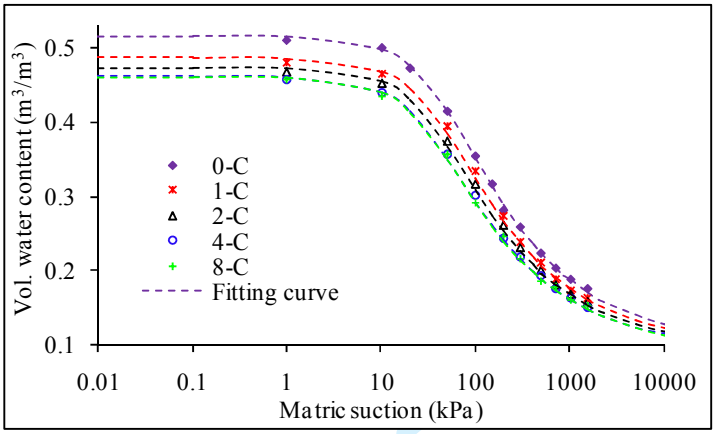

Fig 5. SWCC fitting curve of different drying-wetting cycle samples

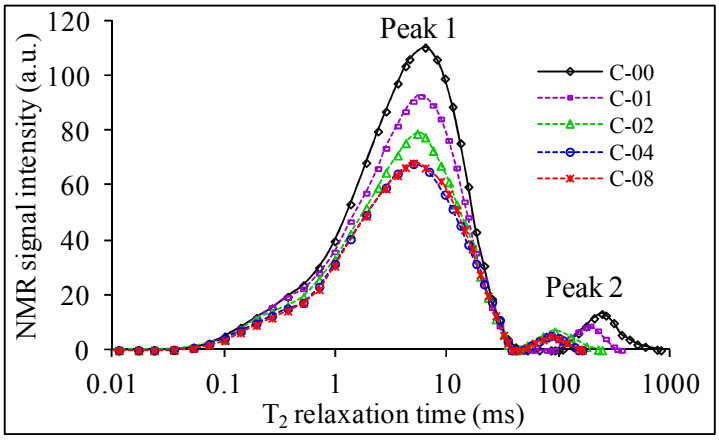

Fig 6. Variation of T_2 distribution curves with respect to drying-wetting cycle

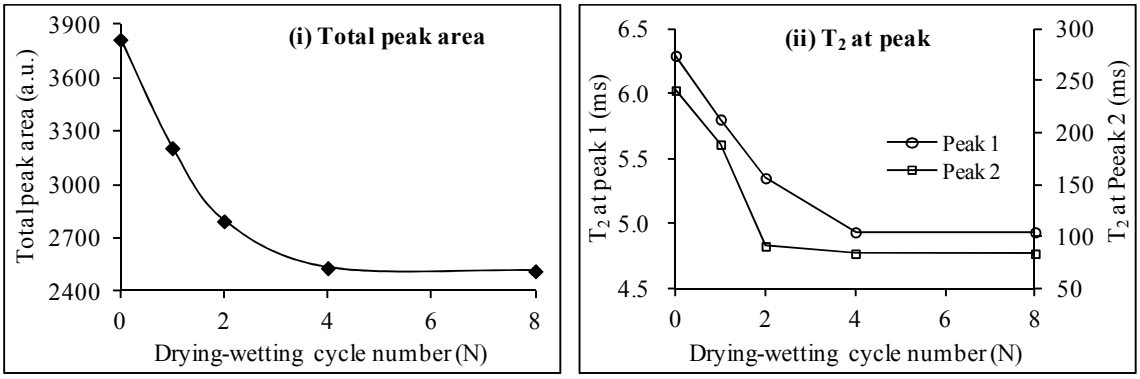

Fig 7. Variations of (i) peak area and (ii) T_2 at peak area with drying-wetting cycles.

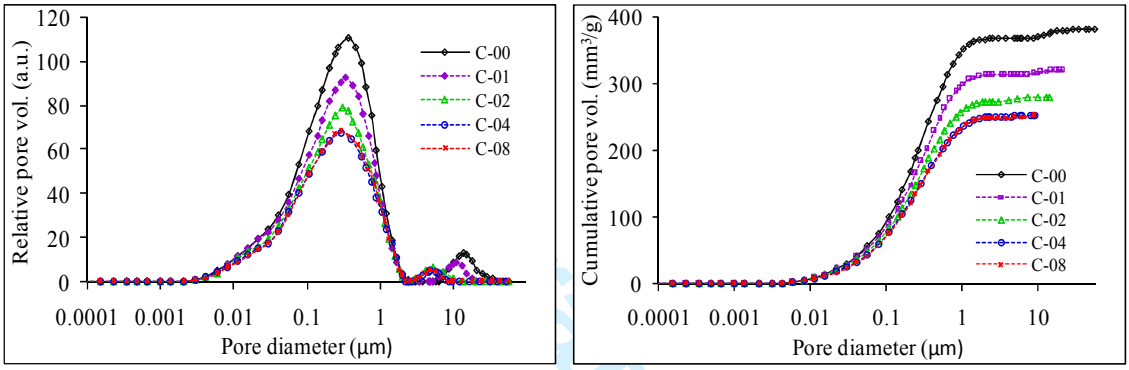

(i) relative pore volume (ii) cumulative pore volume

Fig 8. POSD of drying-wetting cycle samples

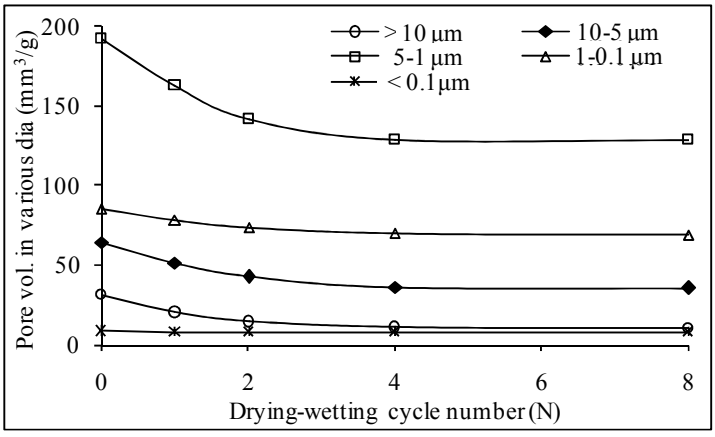

Fig 9. Variations of different pore sizes with wetting-drying cycles

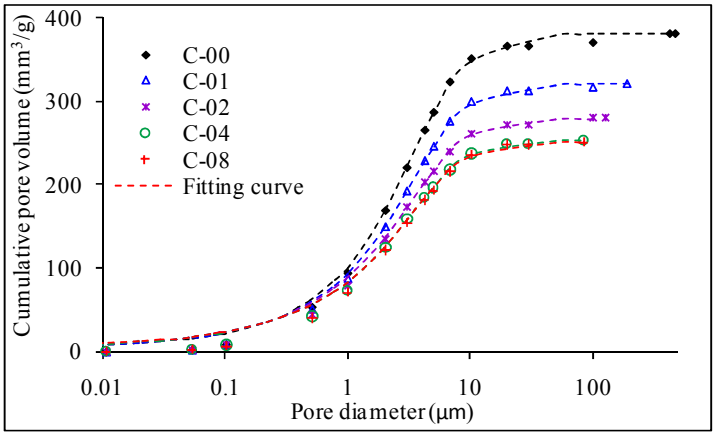

Fig 10. POSD fitting curve of different wetting-drying cycle samples

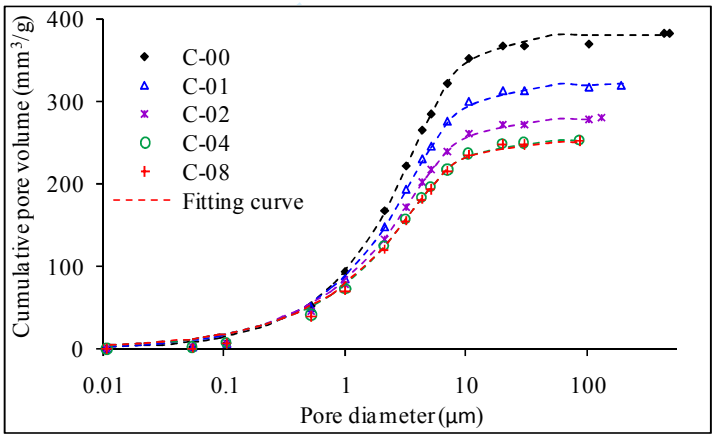

Fig 11. POSD fitting curve of different wetting-drying cycle samples considering V_r= 0.

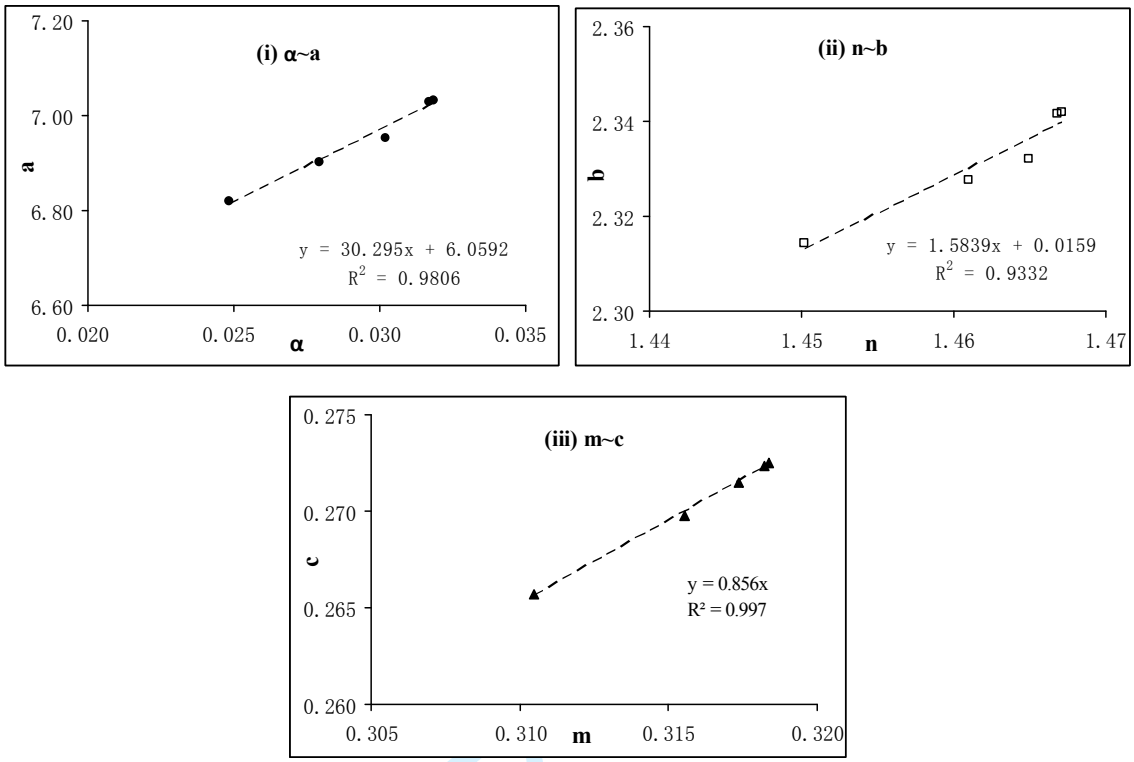

Fig 12. Relationship between the fitting parameters (i) α ~ a, (ii) n ~ b and (iii) m ~ c

List of tables

Table 1. Basic material properties of the tested granite residual soils

Depth	ρ_d	NMC	Atterberg limits			(%)/Free	Grain size (%)			
(m)	(g/cm^3)	%	W_L %	W_P %	I_P %	swell	Gravel	Sand	Silt	Clay
5.7~6.0	1.30	37.20	57.1	30.7	26.40	9.75	4.6	33.4	45.9	16.1

Table 2. SWCC parameters with respect to different drying-wetting cycles

Wet-dry	Fitting parameters (using van Genuchten, 1980)					R^2
Cycle no.	θ_s	θ_r	α	n	m	
0	0.5146	0.0898	0.0248	1.4502	0.3105	0.9924
1	0.4859	0.0880	0.0279	1.4610	0.3155	0.9885
2	0.4727	0.0870	0.0302	1.4649	0.3174	0.9934
4	0.4611	0.0865	0.0317	1.4668	0.3182	0.9907
8	0.4595	0.0864	0.0319	1.4671	0.3184	0.9925

Table 3. POSDs of drying-wetting cycle samples

Wet-dry cycle no.	Total measurable pore vol. (mm^3/g)	Pore vol. with different diameter (mm^3/g)				
		>10μm	10-5μm	5-1μm	1-0.1μm	<0.1μm
C-00	381.49	31.42	64.22	192.30	85.29	8.26
C-01	320.62	20.09	51.63	162.58	78.26	8.05
C-02	279.61	14.44	42.36	141.29	73.71	7.82
C-04	253.17	10.73	36.20	128.85	69.72	7.68
C-08	251.42	10.27	35.60	128.70	69.24	7.62

Table 4. POSD fitting parameters of drying-wetting cycle samples

Wet-dry	POSD fitting parameters					R^2
Cycle no.	V_s	V_r	a	b	c	
0	380.93	1.88	6.7384	2.3201	0.2657	0.9513
1	320.62	1.74	6.9010	2.3277	0.2697	0.9689
2	279.42	1.65	6.9537	2.3322	0.2715	0.9725
4	253.09	1.60	7.0293	2.3506	0.2723	0.9603
8	252.16	1.59	7.0328	2.3520	0.2725	0.9682

Table 5. POSD fitting parameters of drying-wetting cycle samples considering V_r= 0.

Wet-dry Cycle no.	Fitting parameters				R^2
	V_s	a	b	c	
0	380.93	6.7384	2.3201	0.2657	0.9852
1	320.62	6.9010	2.3277	0.2697	0.9838
2	279.42	6.9537	2.3322	0.2715	0.9815
4	253.09	7.0293	2.3506	0.2723	0.9728
8	252.16	7.0328	2.3520	0.2725	0.9764